PERGAMON

International Journal of Solids and Structures 39 (2002) 2893–2909

INTERNATIONAL JOURNAL OF SOLIDS and STRUCTURES

www.elsevier.com/locate/ijsolstr

New accurate efficient modeling techniques for the vibration analysis of T-joint thin-walled box structures

Jin Hong Kim [a], Hyeon Seok Kim [b], Dae Woon Kim [c], Yoon Young Kim [d,*]

[a] *Institute of Advanced Machinery and Design, Seoul National University, South Korea*

[b] *Functional System Test Team 2, Research and Development Division for Hyundai Motor Company and Kia Motors Corporation, South Korea*

[c] *Noise Vibration and Harshness Team, Research and Development Division for Hyundai Motor Company and Kia Motors Corporation, South Korea*

[d] *School of Mechanical and Aerospace Engineering, Seoul National University, San 56-1, Shinlim-Dong, Kwanak-Gu, Seoul 151-742, South Korea*

Received 11 April 2001; received in revised form 14 March 2002

Abstract

We propose new accurate efficient modeling techniques for the vibration analysis of T-joint thin-walled box structures. The essence of the present techniques is to use beam elements to model thin-walled members of the joint, but the elements are based on an eight-degree-of-freedom (8-DOF) beam theory capable of handling warping and distortion. Two approaches are considered to model the interfacing joint region connected to three adjacent thin-walled box structures: the first one is to model the joint region with plate elements and the second one is to use a joint element derived to be consistent with nearby 8-DOF beam elements. The efficiency of the present techniques comes from the use of beam elements to model the box structures while the accuracy comes from the use of the higher-order beam theory accounting for warping and distortion. The procedures to match the dissimilar elements and to develop the joint element are also presented in this work. The effectiveness of the present approaches is demonstrated by numerical examples.

Keywords: Modeling; Vibration; Structures

1. Introduction

Thin-walled beams are widely used in many applications—aerospace, modern architecture, and mechanical structures because of their high rigidity and lightweightness. Recent manufacturing technology allows the use of thin-walled beams with various shapes. Therefore, the optimization and analysis of these structures has been a challenging topic.

* Corresponding author.
E-mail address: yykim@snu.ac.kr (Y.Y. Kim).

0020-7683/02/$ - see front matter
PII: S0020-7683(02)00257-3

Many thin-walled beam theories are based on the classical work by Vlasov (1961). Focusing our attention to the analysis of joints of thin-walled structures, most investigations were mainly concerned with the estimation of joint flexibility. Chang (1974) demonstrated the significance of the flexibility of car body connections by examining static structural responses. Lubkin (1974) treated a tubular welded joint of a vehicle frame. Garro and Vullo (1986) analyzed the dynamic behavior of typical body joints under two typical actual load conditions. They addressed that the plates along weld spots tend to detach from each other when joint deformations occur. Lee and Nikolaidis (1992) proposed a two-dimensional joint model in order to consider joint flexibility, the offset of rotation centers, and coupling effects between the movement of joint branches.

Sunami et al. (1988, 1990) studied the behavior of isolated T- and L-shaped box beams and discussed the significance of shear deformation. El-sayed (1989) calculated the torsional spring rates of structural joints using finite elements. Balch and Steele (1987) performed an asymptotic analysis for T-joint box beam structures. They discussed the decay distance of end effects of thin-walled box beams. Altenbach (1991) and Altenbach et al. (1994) present a generalized theory of thin-walled beams with closed and open cross-sections using n degrees of freedom. The theoretical framework allows the solution of various application problems including T-joint box beam structures and vibrations.

Through many investigations including those cited above, the importance of joint flexibility has been now well recognized, and most practical modeling techniques take the additional flexibility into account using artificial stiffness at the joint area whereas the adjacent structures are modeled by beam elements. Kim et al. (1995) have investigated the practicality of using spring or equivalent beam elements in considering the flexibility. Particularly for vibration analysis, existing modeling techniques using beams and joint elements do not predict accurately the structural behaviors of a joint even for a relatively low frequency range. The main reason for this behavior is that conventional beam elements are not capable of handling warping and distortion that affect significantly the joint flexibility particularly for dynamic situations. To overcome the limitation of the existing beam element-based modeling techniques, we propose new modeling techniques valid for both static and dynamic cases, but with an emphasis on dynamic cases. The essence of the proposed modeling techniques is to employ an eight-degree-of-freedom (8-DOF) beam theory having warping and distortion degrees in addition to conventional six degrees of freedom.

In this work, thin-walled box structures adjacent to a joint region are modeled by the 8-DOF beam theory while the joint region is modeled by two approaches. The first approach is to model the joint region with plate elements. To connect dissimilar plate and beam elements at the interface, we employ a technique based on a pseudo-inverse matrix. The second approach is to model the joint region with a joint element derived to be consistent with 8-DOF beam elements. To estimate the stiffness of the joint element, we impose the deformation pattern expressed by the 8-DOF beam theory on the interfaces of the joint area modeled by plate elements and calculate the reaction forces on all the interfaces encompassing the joint region.

Numerical results show an excellent agreement between the present predictions and those by the detailed plate finite element analysis. Although the present investigation is limited to box beams, the present method can be extended to handle joints consisting of complicated cross-sections, and thus will be expected to play an important role in an early structural design such as an initial automobile body design.

2. Eight-degree-of-freedom thin-walled box beam theory

The underlying difference of the present modeling technique with existing modeling techniques of a T-joint structure is to use a higher-order beam theory including warping and distortional deformations.

Kim and Kim (1999a, 2000) have developed a one-dimensional beam theory to deal with coupled deformations of torsion, warping and distortion in thin-walled general sectioned beams. By including ex-

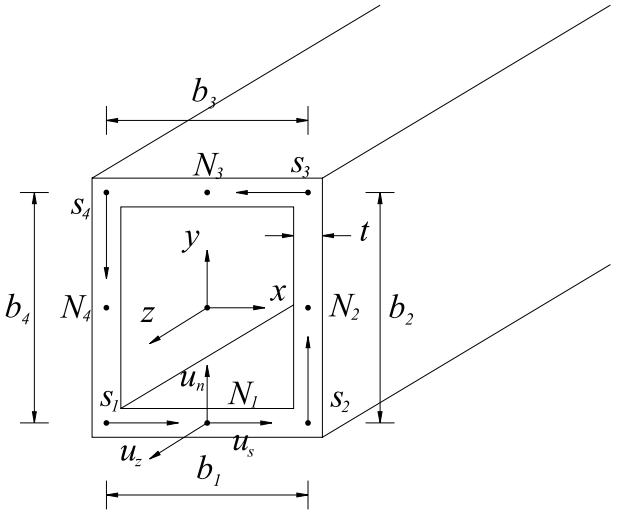

Fig. 1. Geometry of a thin-walled rectangular cross-section (N_i: a generic point on the ith wall to which ON_i is normal) ($b_1 = b_3 = b,\ b_2 = b_4 = h$).

tensional and flexural deformations in addition to the coupled deformations, an 8-DOF one-dimensional thin-walled box beam theory is derived here.

Fig. 1 shows the geometry of a thin-walled beam having a rectangular cross-section. It is assumed that the wall thickness t is much smaller than the beam length. The tangential coordinate s is measured along the contour of the cross-section, and different origins are used for each wall. The normal coordinate n directs outwards from the contour. The displacements of a point on the middle line of the wall are expressed in terms of the normal u_n, tangential u_s and axial u_z components as indicated in Fig. 1.

Eight degrees of freedom considered in the present theory consist of three translations (u, v, w) along x-, y-, z-axes, three rotations (θ_x, θ_y, θ_z) about x-, y-, z-axes, warping ω and distortion χ. The corresponding deformations of the section contour are depicted in Fig. 2.

Denoting the section deformations of the contour by $\psi(s)$, the shell displacements of the contour can be written as

$$u_s(s,z) = \psi_s^u(s)u(z) + \psi_s^v(s)v(z) + \psi_s^{\theta_z}(s)\theta_z(z) + \psi_s^{\chi}(s)\chi(z) \tag{1}$$

$$u_n(s,z) = \psi_n^u(s)u(z) + \psi_n^v(s)v(z) + \psi_n^{\theta_z}(s)\theta_z(z) + \psi_n^{\chi}(s)\chi(z) \tag{2}$$

$$u_z(s,z) = \psi_z^{\theta_x}(s)\theta_x(z) + \psi_z^{\theta_y}(s)\theta_y(z) + \psi_z^{w}(s)w(z) + \psi_z^{\omega}(s)\omega(z) \tag{3}$$

Note that the subscripts n, s and z denote the directions of the displacement.

The nonvanishing components (ψ^u, ψ^v, ψ^{θ_x}, ψ^{θ_y}, ψ^w) of the section deformation shape are straightforward to write:

$$\psi_s^u(s_i) = \cos\alpha_i, \quad \psi_n^u(s_i) = -\sin\alpha_i,$$
$$\psi_s^v(s_i) = \sin\alpha_i, \quad \psi_n^v(s_i) = \cos\alpha_i,$$
$$\psi_z^{\theta_y}(s_i) = -x, \quad \psi_z^{\theta_x}(s_i) = y, \quad \psi_z^w = 1$$

where α_i is the angle between the x-axis and the s_i axis attached to the ith wall. The nonvanishing section deformations associated with the rotation $\theta(z)$ about the z-axis are

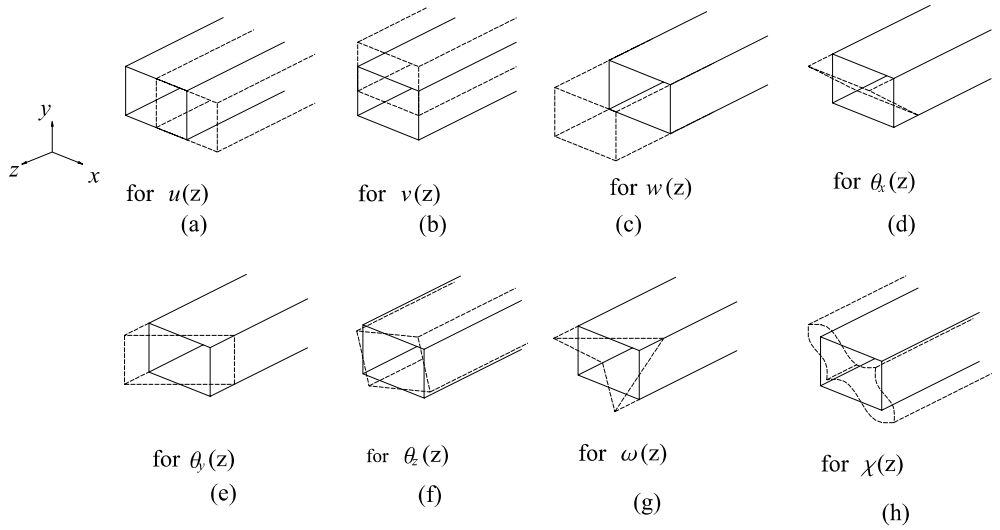

Fig. 2. Deformation shapes of a box beam section corresponding to eight degrees of freedom (those depicted in (a–f) are considered in a standard six-degree-of-freedom beam theory).

$$\psi_s^{\theta_z}(s_i) = r(s_i)\ (r(s_i) = r_i = h/2 \quad \text{for } i = 1,3; \quad b/2 \text{ for } i = 2,4)$$
$$\psi_n^{\theta_z}(s_i) = -\frac{b_i}{2} + s_i$$

For the warping deformation $\omega(z)$, only the axial displacement component is nonvanishing

$$\psi_z^{\omega}(s_i) = x(s_i)y(s_i) \tag{4}$$

Note that the average axial displacement due to Eq. (4) vanishes.

Following the procedure used in Kim and Kim (1999a), the nonvanishing section deformations corresponding to distortion $\chi(z)$ are shown to be

$$\begin{aligned}\psi_n^{\chi}(s_1) = \psi_n^{\chi}(s_3) &= \frac{bh}{b+h}\left[-4m_1(s_1/b)^3 + 6m_1(s_1/b)^2 - 2(m_1-1)(s_1/b) - 1\right] \\ \psi_n^{\chi}(s_2) = \psi_n^{\chi}(s_4) &= \frac{bh}{b+h}\left[4m_2(s_2/h)^3 - 6m_2(s_2/h)^2 + 2(m_2-1)(s_2/h) + 1\right]\end{aligned} \tag{5}$$

where

$$m_1 = \frac{b}{h}, \quad m_2 = \frac{h}{b}$$

The tangential component ψ_s^{χ} of the distortion can be written as

$$\psi_s^{\chi}(s_i) = \frac{bh}{b+h}(-1)^i \tag{6}$$

Using the shell displacements of the section contour defined in Eqs. (1)–(3) one can approximate the three-dimensional displacements (u_s, u_n, u_z) for $n \neq 0$ as

$$
\begin{aligned}
u_s(n,s,z) &\approx u_s(s,z) - n\frac{\partial u_n(s,z)}{\partial s} = \psi_s^u(s)u(z) + \psi_s^v(s)v(z) + \psi_s^{\theta_z}(s)\theta_z(z) + \psi_s^{\chi}(s)\chi(z) - n\frac{\mathrm{d}\psi_n^{\chi}(s)}{\mathrm{d}s}\chi(z)\\
u_n(n,s,z) &\approx u_n(s,z) = \psi_n^u(s)u(z) + \psi_n^v(s)v(z) + \psi_n^{\theta_z}(s)\theta_z(z) + \psi_n^{\chi}(s)\chi(z)\\
u_z(n,s,z) &\approx u_z(s,z) = \psi_z^{\theta_x}(s)\theta_x(z) + \psi_z^{\theta_y}(s)\theta_y(z) + \psi_z^{w}(s)w(z) + \psi_z^{\omega}(s)\omega(z)
\end{aligned}
\tag{7}
$$

The three-dimensional strain components can be determined from the displacement field given by Eq. (7):

$$
\begin{aligned}
\epsilon_{zz} &= \psi_z^w(s)\frac{\mathrm{d}w(z)}{\mathrm{d}z} + \psi_z^{\theta_x}(s)\frac{\mathrm{d}\theta_x(z)}{\mathrm{d}z} + \psi_z^{\theta_y}(s)\frac{\mathrm{d}\theta_y(z)}{\mathrm{d}z} + \psi_z^{\omega}(s)\frac{\mathrm{d}\omega(z)}{\mathrm{d}z}\\
\epsilon_{zs} &\approx \frac{1}{2}\left[\psi_s^u(s)\frac{\mathrm{d}u(z)}{\mathrm{d}z} + \psi_s^v(s)\frac{\mathrm{d}v(z)}{\mathrm{d}z} + \frac{\mathrm{d}\psi_z^{\theta_x}(s)}{\mathrm{d}s}\theta_x(z) + \frac{\mathrm{d}\psi_z^{\theta_y}(s)}{\mathrm{d}s}\theta_y(z) + \psi_s^{\theta_z}(s)\frac{\mathrm{d}\theta_z(z)}{\mathrm{d}z} + \frac{\mathrm{d}\psi_z^{\omega}(s)}{\mathrm{d}s}\omega(z)\right.\\
&\quad \left. + \psi_s^{\chi}(s)\frac{\mathrm{d}\chi(z)}{\mathrm{d}z}\right]\\
\epsilon_{ss} &= n\frac{\mathrm{d}^2\psi_n^{\chi}}{\mathrm{d}s^2}\chi(z)
\end{aligned}
\tag{8}
$$

Other strain components are negligible in comparison with these components. We remark that the four terms in ϵ_{zs} in Eq. (8) become

$$
\psi_s^u(s)\frac{\mathrm{d}u(z)}{\mathrm{d}z} + \psi_s^v(s)\frac{\mathrm{d}v(z)}{\mathrm{d}z} + \frac{\mathrm{d}\psi_z^{\theta_x}(s)}{\mathrm{d}s}\theta_x(z) + \frac{\mathrm{d}\psi_z^{\theta_y}(s)}{\mathrm{d}s}\theta_y(z) = \psi_s^u(s)\left[\frac{\mathrm{d}u(z)}{\mathrm{d}z} - \theta_y(z)\right] + \psi_s^v(s)\left[\frac{\mathrm{d}v(z)}{\mathrm{d}z} - \theta_x(z)\right]
$$

where $\mathrm{d}\psi_z^{\theta_y}/\mathrm{d}s = -\psi_s^u$ and $\mathrm{d}\psi_z^{\theta_x}/\mathrm{d}s = -\psi_s^v$ are used (see Fig. 2). These terms are used to represent the shear terms when nonuniform bending occurs.

Nonvanishing stress components are determined from the following constitutive relation

$$
\sigma_{zz} = E_1(\epsilon_{zz} + v\epsilon_{ss}), \quad \sigma_{ss} = E_1(\epsilon_{ss} + v\epsilon_{zz}), \quad \sigma_{sz} = 2G\epsilon_{sz} \tag{9}
$$

with $E_1 = E/(1-v^2)$ where E and G are Young's and shear moduli, respectively and v is Poisson's ratio.

To derive the present 8-DOF beam theory, the potential energy expressed in three-dimensional quantities will be integrated over the beam cross-section A. Since we will follow the same procedure employed in Kim and Kim (1999a,b, 2000), the detailed analysis will be omitted here. The final form of the system potential energy in its one-dimensional form is

$$
\begin{aligned}
\Pi &= \frac{1}{2}E\int [Aw'^2 + I_{xx}\theta_x'^2 + I_{yy}\theta_y'^2 + I_{\omega\omega}\omega'^2 + 2\{I_{wx}w'\theta_x' + I_{wy}w'\theta_y' + I_{w\omega}w'\omega' + I_{xy}\theta_x'\theta_y' + I_{x\omega}\theta_x'\omega' + I_{y\omega}\theta_y'\omega'\}]\,\mathrm{d}z\\
&\quad + \frac{1}{2}G\int [b_1u'^2 + b_2v'^2 + b_3\theta_x^2 + b_4\theta_y^2 + b_5\theta_z'^2 + b_6\omega^2 + b_7\chi'^2 + 2\{b_8u'v' + b_9u'\theta_x + b_{10}u'\theta_y + b_{11}u'\theta_z'\\
&\quad + b_{12}u'\omega + b_{13}u'\chi' + b_{14}v'\theta_x + b_{15}v'\theta_y + b_{16}v'\theta_z' + b_{17}v'\omega + b_{18}v'\chi' + b_{19}\theta_x\theta_y + b_{20}\theta_x\theta_z' + b_{21}\theta_x\omega\\
&\quad + b_{22}\theta_x\chi' + b_{23}\theta_x\theta_z' + b_{24}\theta_y\omega + b_{25}\theta_y\chi' + b_{26}\theta_z'\omega + b_{27}\theta_z'\chi' + b_{28}\omega\chi'\}]\,\mathrm{d}z\\
&\quad + \frac{1}{2}E\int c\chi^2\,\mathrm{d}z + \int [m_x\theta_x + m_y\theta_y + f_zw + B\omega + f_xu + f_yv + m_z\theta_z + Q\chi]\,\mathrm{d}z
\end{aligned}
\tag{10}
$$

where $()'$ denotes the differentiation with respect to z. Constants $b_1, \ldots$, etc. may be found as

$$
\begin{aligned}
&A = \int (\psi_z^w)^2 \,\mathrm{d}A, \quad I_{xx} = \int y^2 \,\mathrm{d}A, \quad I_{yy} = \int x^2 \,\mathrm{d}A, \quad I_{\omega\omega} = \int \omega^2 \,\mathrm{d}A \\
&I_{xy} = \int -xy \,\mathrm{d}A, \quad I_{x\omega} = \int y\omega \,\mathrm{d}A, \quad I_{y\omega} = \int -x\omega \,\mathrm{d}A \\
&b_1 = \int (\psi_s^u)^2 \,\mathrm{d}A, \quad b_2 = \int (\psi_s^v)^2 \,\mathrm{d}A, \quad b_3 = \int \left(\frac{\mathrm{d}\psi_z^{\theta_x}}{\mathrm{d}s}\right)^2 \mathrm{d}A, \quad b_4 = \int \left(\frac{\mathrm{d}\psi_z^{\theta_y}}{\mathrm{d}s}\right)^2 \mathrm{d}A \\
&b_5 = \int (\psi_z^{\theta_y})^2 \,\mathrm{d}A, \quad b_6 = \int \left(\frac{\mathrm{d}\psi_z^{\omega}}{\mathrm{d}s}\right)^2 \mathrm{d}A, \quad b_7 = \int (\psi_z^{\chi})^2 \,\mathrm{d}A, \quad b_8 = \int \psi_s^u \psi_s^v \,\mathrm{d}A \\
&b_9 = \int \psi_s^u \frac{\mathrm{d}\psi_z^{\theta_x}}{\mathrm{d}s} \,\mathrm{d}A, \quad b_{10} = \int \psi_s^u \frac{\mathrm{d}\psi_z^{\theta_y}}{\mathrm{d}s} \,\mathrm{d}A, \quad b_{11} = \int \psi_s^u \psi_s^{\theta_z} \,\mathrm{d}A \\
&b_{12} = \int \psi_s^u \frac{\mathrm{d}\psi_z^{\omega}}{\mathrm{d}s} \,\mathrm{d}A, \quad b_{13} = \int \psi_s^u \psi_s^{\chi} \,\mathrm{d}A, \quad b_{14} = \int \psi_s^v \frac{\mathrm{d}\psi_z^{\theta_x}}{\mathrm{d}s} \,\mathrm{d}A \\
&b_{15} = \int \psi_s^v \frac{\mathrm{d}\psi_z^{\theta_y}}{\mathrm{d}s} \,\mathrm{d}A, \quad b_{16} = \int \psi_s^v \psi_s^{\theta_z} \,\mathrm{d}A, \quad b_{17} = \int \psi_s^v \frac{\mathrm{d}\psi_z^{\omega}}{\mathrm{d}s} \,\mathrm{d}A \\
&b_{18} = \int \psi_s^v \psi_s^{\chi} \,\mathrm{d}A, \quad b_{19} = \int \frac{\mathrm{d}\psi_z^{\theta_x}}{\mathrm{d}s} \frac{\mathrm{d}\psi_z^{\theta_y}}{\mathrm{d}s} \,\mathrm{d}A, \quad b_{20} = \int \frac{\mathrm{d}\psi_z^{\theta_x}}{\mathrm{d}s} \psi_s^{\theta_z} \,\mathrm{d}A \\
&b_{21} = \int \frac{\mathrm{d}\psi_z^{\theta_x}}{\mathrm{d}s} \frac{\mathrm{d}\psi_z^{\omega}}{\mathrm{d}s} \,\mathrm{d}A, \quad b_{22} = \int \frac{\mathrm{d}\psi_z^{\theta_x}}{\mathrm{d}s} \psi_s^{\chi}, \quad b_{23} = \int \frac{\mathrm{d}\psi_z^{\theta_y}}{\mathrm{d}s} \psi_s^{\theta_z} \,\mathrm{d}A \\
&b_{24} = \int \frac{\mathrm{d}\psi_z^{\theta_y}}{\mathrm{d}s} \frac{\mathrm{d}\psi_z^{\omega}}{\mathrm{d}s} \,\mathrm{d}A, \quad b_{25} = \int \frac{\mathrm{d}\psi_z^{\theta_y}}{\mathrm{d}s} \psi_s^{\chi} \,\mathrm{d}A, \quad b_{26} = \int \psi_s^{\theta_z} \frac{\mathrm{d}\psi_z^{\omega}}{\mathrm{d}s} \,\mathrm{d}A \\
&b_{27} = \int \psi_s^{\theta_z} \psi_s^{\chi} \,\mathrm{d}A, \quad b_{28} = \int \frac{\mathrm{d}\psi_z^{\omega}}{\mathrm{d}s} \psi_s^{\chi} \,\mathrm{d}A, \quad c = \int \left(n \frac{\mathrm{d}^2\psi_n^{\chi}}{\mathrm{d}s^2}\right)^2 \mathrm{d}A
\end{aligned}
\tag{11}
$$

One-dimensional load terms, such as m_x, are defined as

$$
\begin{aligned}
&m_x = \int p_z \psi_z^{\theta_x} \,\mathrm{d}A, \quad m_y = \int p_z \psi_z^{\theta_y} \,\mathrm{d}A, \quad f_z = \int p_z \psi_z^{w} \,\mathrm{d}A, \quad B = \int p_z \psi_z^{\omega} \,\mathrm{d}A \\
&f_x = \int p_x \,\mathrm{d}A, \quad f_y = \int p_y \,\mathrm{d}A, \quad m_z = \int p_s \psi_s^{\theta_z} \,\mathrm{d}A, \quad Q = \int p_s \psi_s^{\chi} \,\mathrm{d}A
\end{aligned}
\tag{12}
$$

where p_z, p_x, p_y and p_s denote z, x, y and s directional distributive loads, respectively. The symbols B and Q in Eq. (12) define the bimoment and the transverse bimoment, respectively (see Vlasov, 1961).

In the case of vibration problems, the Lagrangian $L = T - \Pi$ is used where the kinetic energy T is given by

$$
\begin{aligned}
T &= \frac{1}{2} \int [u_s^2 + u_n^2 + u_z^2] \rho \,\mathrm{d}s \,\mathrm{d}n \,\mathrm{d}z \\
&= \frac{1}{2} \int \left[b_1 u^2 + b_2 v^2 + b_5 \theta_z^2 + b_7 \chi^2 + d_0 \chi^2 + 2\{ b_8 uv + b_{11} u\theta_z + b_{13} u\chi + b_{16} v\theta_z + b_{18} v\chi + b_{27} \theta_z \chi \} m \,\mathrm{d}z \right. \\
&\quad + \frac{1}{2} \int \left[d_1 u^2 + d_2 v^2 + d_3 \theta_z^2 + d_4 \chi^2 + 2\{ d_5 uv + d_6 u\theta_z + d_7 u\chi + d_8 v\theta_z + d_9 v\chi + d_{10} \theta_z \chi \} \right] m \,\mathrm{d}z \\
&\quad + \frac{1}{2} \int [I_{xx} \theta_x^2 + I_{yy} \theta_y^2 + Aw^2 + I_{\omega\omega} \omega^2] m \,\mathrm{d}z
\end{aligned}
\tag{13}
$$

where ρ and m denote the mass density and mass per unit length, respectively. In Eq. (13), d_1, etc. are defined as

$$
\begin{aligned}
&d_0 = \int \left(n \frac{\mathrm{d}\psi_n^{\chi}}{\mathrm{d}s} \right)^2 \mathrm{d}A, \quad d_1 = \int (\psi_n^u)^2 \, \mathrm{d}A, \quad d_2 = \int (\psi_n^v)^2 \, \mathrm{d}A \\
&d_3 = \int (\psi_n^{\theta_z})^2 \, \mathrm{d}A, \quad d_4 = \int (\psi_n^{\chi})^2 \, \mathrm{d}A, \quad d_5 = \int \psi_n^u \psi_n^v \, \mathrm{d}A \\
&d_6 = \int \psi_n^u \psi_n^{\theta_z} \, \mathrm{d}A, \quad d_7 = \int \psi_n^u \psi_n^{\chi} \, \mathrm{d}A, \quad d_8 = \int \psi_n^v \psi_n^{\theta_z} \, \mathrm{d}A \\
&d_9 = \int \psi_n^v \psi_n^{\chi} \, \mathrm{d}A, \quad d_{10} = \int \psi_n^{\theta_z} \psi_n^{\chi} \, \mathrm{d}A
\end{aligned}
\tag{14}
$$

3. Joint modeling techniques

To develop an accurate efficient model of a T-joint structure, 8-DOF beam elements are used to model three thin-walled box beams adjacent to the joint region defined in Fig. 3. The effects of the size of the joint region will be also numerically investigated in the next section. We will consider two approaches to model the joint region. The first approach, which will be discussed in Section 3.1, is to model it with plate elements and match dissimilar elements at the interface using a pseudo-inverse matrix. The second approach is to generate a joint element from the plate element model of the joint region in such a way that its degrees of freedom are consistent with those of 8-DOF beams.

Unlike typical modeling techniques using 6-DOF beam elements for the adjacent box beams, the use of 8-DOF beam elements having the additional degrees of freedom for warping and distortion requires careful considerations of the kinematic relations and the equilibrium consideration.

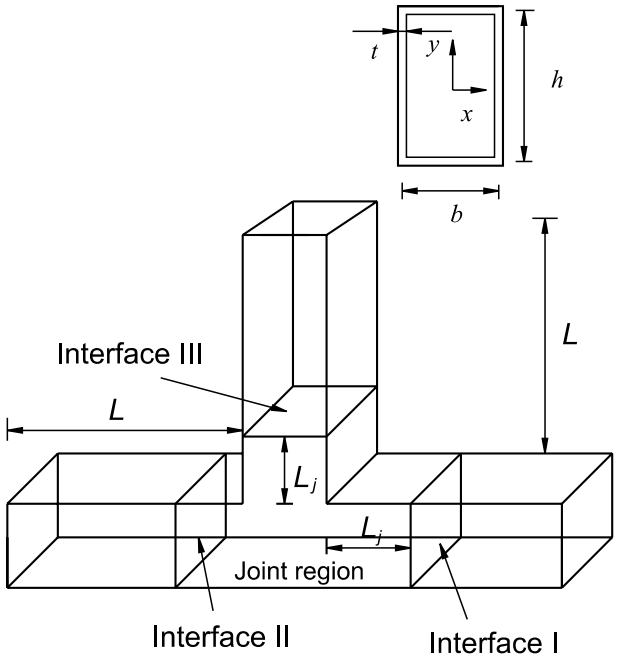

Fig. 3. A T-joint thin-walled structure.

3.1. The joint region modeled by plate elements

The joint region in Fig. 3 is modeled by plate elements and its adjacent box beams by 8-DOF beams. The main task is now to match the dissimilar elements on the interfaces. The number of degrees of freedom used to represent the interfacing part of the joint region is

$$N^j \times N_d$$

where N^j is the total number of nodes of plate elements at the jth interface ($j = \mathrm{I}, \mathrm{II}, \mathrm{III}$; see Fig. 3). The number of nodal degrees of freedom for the interface plate element is denoted by N_d.

Though plate elements have rotational degrees, only three translational degrees of freedom are considered at the interface and thus $N_d = 3$, here (see Kim, 1997). Accordingly, we consider the following displacement vector representing the interface degrees of freedom for the region modeled by plates (see Fig. 4).

$$\mathbf{D}^j = \left(U^j_{x1}, U^j_{y1}, U^j_{z1}, \ldots, U^j_{xNj}, U^j_{yNj}, U^j_{zNj}\right)^{\mathrm{T}} \tag{15}$$

The subscripts x, y and z denote the directions of displacement components and the superscript j represents the interface locations. The interface degrees of freedom for the thin-walled beam structures are denoted by

$$\mathbf{d}^j = \left(u^j, v^j, w^j, \theta^j_x, \theta^j_y, \theta^j_z, \omega^j, \chi^j\right)^{\mathrm{T}} \tag{16}$$

One can determine a transformation matrix $\mathbf{T}_j$ relating $\mathbf{d}^j$ and $\mathbf{D}^j$ as

$$\mathbf{D}^j = \mathbf{T}_j \mathbf{d}^j \tag{17}$$

The detailed expression for $\mathbf{T}_j$ will be given later. If the inverse matrix of $\mathbf{T}_j$ exists, $\mathbf{d}^j$ can be easily determined from $\mathbf{D}^j$.

$$\mathbf{d}^j = \mathbf{T}_j^{-1} \mathbf{D}^j \tag{18}$$

Since the matrix $\mathbf{T}_j$ is not a square matrix, the direct inverse matrix $\mathbf{T}_j^{-1}$ cannot be obtained. To resolve this matter, we propose to use the pseudo-inverse matrix $\mathbf{T}_j^{+}$ such that

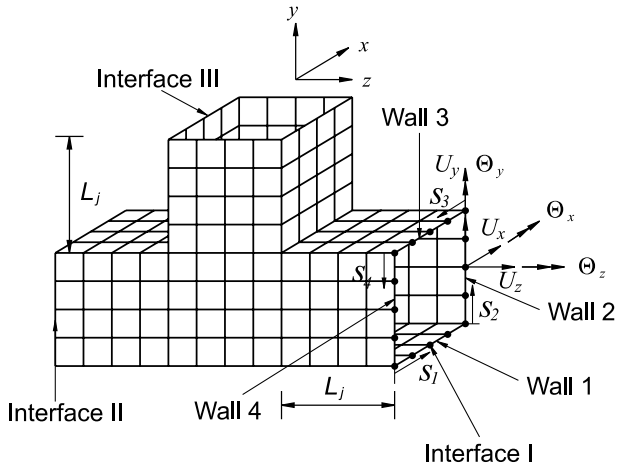

Fig. 4. Plate finite element model of a T-joint thin-walled structure.

$$\mathbf{d}^j = \mathbf{T}_j^+ \mathbf{D}^j \tag{19}$$

where $\mathbf{T}_j^+$ can be determined as (see, e.g., Bjerhammar, 1973)

$$\mathbf{T}_j^+ = (\mathbf{T}_j^{\mathrm{T}} \mathbf{T}_j)^{-1} \mathbf{T}_j^{\mathrm{T}}$$

Next, we can derive the relation between the force vector $\mathbf{f}^j$ of the beam elements and the force vector $\mathbf{F}^j$ of plate elements at the interface. By imposing the condition that the virtual work done by $\mathbf{F}^j$ through the virtual displacement $\delta\mathbf{D}^j$ must be equal to the virtual work done by $\mathbf{f}^j$ through $\delta\mathbf{d}^j$, the following equation is obtained:

$$\mathbf{F}^{j^{\mathrm{T}}} \delta\mathbf{D}^j = \mathbf{f}^{j^{\mathrm{T}}} \delta\mathbf{d}^j \tag{20}$$

Substituting Eq. (19) into Eq. (20) yields the following relationship between $\mathbf{f}^j$ and $\mathbf{F}^j$.

$$\mathbf{F}^j = (\mathbf{T}_j^+)^{\mathrm{T}} \mathbf{f}^j \tag{21}$$

$$\mathbf{f}^j = \mathbf{T}_j^{\mathrm{T}} \mathbf{F}^j \tag{22}$$

Eqs. (19)–(22) will be used to match interface conditions.

To find the governing equations for a whole T-joint structure, we first write the equations of motion for the joint region modeled by plate elements:

$$\begin{bmatrix} \mathbf{M}_{ii} & \mathbf{M}_{ij} \\ \mathbf{M}_{ji} & \mathbf{M}_{jj} \end{bmatrix} \cdot \begin{Bmatrix} \ddot{\mathbf{D}}^i \\ \ddot{\mathbf{D}}^j \end{Bmatrix} + \begin{bmatrix} \mathbf{K}_{ii} & \mathbf{K}_{ij} \\ \mathbf{K}_{ji} & \mathbf{K}_{jj} \end{bmatrix} \cdot \begin{Bmatrix} \mathbf{D}^i \\ \mathbf{D}^j \end{Bmatrix} = \begin{Bmatrix} \mathbf{F}^i \\ \mathbf{F}^j \end{Bmatrix} \tag{23}$$

where $\mathbf{K}$ and $\mathbf{M}$ denote the stiffness and mass matrices of the joint region, respectively and ($\ddot{}$) denotes the second derivatives with respect to time. In Eq. (23), the superscript i denotes internal quantities that are not associated with the joint interface. Likewise, the governing equations of motion for adjacent box beams are written as

$$\begin{bmatrix} \mathbf{m}_{ii} & \mathbf{m}_{ij} \\ \mathbf{m}_{ji} & \mathbf{m}_{jj} \end{bmatrix} \cdot \begin{Bmatrix} \ddot{\mathbf{d}}^i \\ \ddot{\mathbf{d}}^j \end{Bmatrix} + \begin{bmatrix} \mathbf{k}_{ii} & \mathbf{k}_{ij} \\ \mathbf{k}_{ji} & \mathbf{k}_{jj} \end{bmatrix} \cdot \begin{Bmatrix} \mathbf{d}^i \\ \mathbf{d}^j \end{Bmatrix} = \begin{Bmatrix} \mathbf{f}^i \\ \mathbf{f}^j \end{Bmatrix} \tag{24}$$

where $\mathbf{k}$ and $\mathbf{m}$ denote the stiffness and mass matrices of the box beams, respectively.

Note that the number of degrees of freedom for $\mathbf{d}^j$ is always smaller than the number of the degrees of freedom for $\mathbf{D}^j$. Therefore it is convenient to express $\mathbf{D}^j$ in term of $\mathbf{d}^j$ before combining Eqs. (23) and (24) using

$$\begin{Bmatrix} \mathbf{D}^i \\ \mathbf{D}^j \end{Bmatrix} = [\mathbf{T}] \begin{Bmatrix} \mathbf{D}^i \\ \mathbf{d}^j \end{Bmatrix} \tag{25}$$

where

$$[\mathbf{T}] = \begin{bmatrix} \mathbf{I} & 0 \\ 0 & \mathbf{T}_j \end{bmatrix}, \quad \mathbf{I} = \text{identity matrix}$$

Substituting Eq. (25) into Eq. (23) and pre-multiplying $\mathbf{T}^{\mathrm{T}}$, the following equation is obtained.

$$\begin{bmatrix} \mathbf{M}_{ii} & \mathbf{M}_{ij}\mathbf{T}_j \\ \mathbf{T}_j^{\mathrm{T}}\mathbf{M}_{ji} & \mathbf{T}_j^{\mathrm{T}}\mathbf{M}_{jj}\mathbf{T}_j \end{bmatrix} \cdot \begin{Bmatrix} \ddot{\mathbf{D}}^i \\ \ddot{\mathbf{d}}^j \end{Bmatrix} + \begin{bmatrix} \mathbf{K}_{ii} & \mathbf{K}_{ij}\mathbf{T}_j \\ \mathbf{T}_j^{\mathrm{T}}\mathbf{K}_{ji} & \mathbf{T}_j^{\mathrm{T}}\mathbf{K}_{jj}\mathbf{T}_j \end{bmatrix} \cdot \begin{Bmatrix} \mathbf{D}^i \\ \mathbf{d}^j \end{Bmatrix} = \begin{Bmatrix} \mathbf{F}^i \\ \mathbf{f}_s^j \end{Bmatrix} \tag{26}$$

where $\mathbf{f}_s^j = \mathbf{T}_j^{\mathrm{T}} \mathbf{F}^j$. Combining Eqs. (24) and (26) and setting that $\mathbf{f}^j + \mathbf{f}_s^j = \tilde{\mathbf{f}}^j$, the final equation of motion of the entire T-joint structure can be obtained as

$$\begin{bmatrix} \mathbf{M}_{ii} & \mathbf{M}_{ij}\mathbf{T}_j & 0 \\ \mathbf{T}_j^{\mathrm{T}}\mathbf{M}_{ji} & \mathbf{T}_j^{\mathrm{T}}\mathbf{M}_{jj}\mathbf{T}_j + \mathbf{m}_{jj} & \mathbf{m}_{ji} \\ 0 & \mathbf{m}_{ij} & \mathbf{m}_{ii} \end{bmatrix} \cdot \begin{Bmatrix} \ddot{\mathbf{D}}^i \\ \ddot{\mathbf{d}}^j \\ \ddot{\mathbf{d}}^i \end{Bmatrix} + \begin{bmatrix} \mathbf{K}_{ii} & \mathbf{K}_{ij}\mathbf{T}_j & 0 \\ \mathbf{T}_j^{\mathrm{T}}\mathbf{K}_{ji} & \mathbf{T}_j^{\mathrm{T}}\mathbf{K}_{jj}\mathbf{T}_j + \mathbf{k}_{jj} & \mathbf{k}_{ji} \\ 0 & \mathbf{k}_{ij} & \mathbf{k}_{ii} \end{bmatrix} \cdot \begin{Bmatrix} \mathbf{D}^i \\ \mathbf{d}^j \\ \mathbf{d}^i \end{Bmatrix} = \begin{Bmatrix} \mathbf{F}^i \\ \tilde{\mathbf{f}}^j \\ \mathbf{f}^i \end{Bmatrix} \tag{27}$$

Note that $\mathbf{m}_{ij} = \mathbf{m}_{ji}$ ($\mathbf{M}_{ij} = \mathbf{M}_{ji}$) and $\mathbf{k}_{ij} = \mathbf{k}_{ji}$ ($\mathbf{K}_{ij} = \mathbf{K}_{ji}$).

3.1.1. Derivation of the transformation matrix $\mathbf{T}_j$ ($j =$ I, II and III)

To complete the governing Eq. (27), the transformation matrix $\mathbf{T}_j$ should be determined. Here, we derive the transformation matrix $\mathbf{T}_{\mathrm{I}}$ since $\mathbf{T}_{\mathrm{II}}$ and $\mathbf{T}_{\mathrm{III}}$ can be equally handled.

At Wall 1 of Interface I for $0 \leqslant s_1 \leqslant b_1$ (see Fig. 4), the three displacement components at the ith node of the joint region (modeled by plate elements) can be determined if the 8-DOF beam displacements $(u, v, w, \theta_x, \theta_y, \theta_z, \chi, \omega)$ are known:

$$\begin{aligned} U^{\mathrm{I}}_{x_i} &= u + \frac{h}{2}\theta_z - \frac{bh}{b+h}\chi \\ U^{\mathrm{I}}_{y_i} &= v + x_i\theta_z + \frac{bh}{b+h}\left\{ -\frac{4b}{h}\left(\frac{x_i}{b}\right)^3 + \left(\frac{b}{h}+2\right)\left(\frac{x_i}{b}\right)\right\}\chi \\ U^{\mathrm{I}}_{z_i} &= w - \frac{h}{2}\theta_x - x_i\theta_y - x_i\frac{h}{2}\omega \\ i &= 1, \ldots, N_1^{\mathrm{I}} \end{aligned} \tag{28}$$

where x_i and y_i denote the x and y coordinates measured from the ith node. The number of the nodes at Wall 1 of Interface I is denoted by N_1^{I}.

Similarly for Wall 2 of the Interface I ($0 \leqslant s_2 \leqslant b_2$), we find

$$\begin{aligned} U^{\mathrm{I}}_{x_i} &= u - y_i\theta_z + \frac{bh}{b+h}\left\{ \frac{4h}{b}\left(\frac{y_i}{h}\right)^3 - \left(\frac{h}{b}+2\right)\left(\frac{y_i}{h}\right)\right\}\chi \\ U^{\mathrm{I}}_{y_i} &= v + \frac{b}{2}\theta_z + \frac{bh}{b+h}\chi \\ U^{\mathrm{I}}_{z_i} &= w + y_i\theta_x - \frac{b}{2}\theta_y + y_i\frac{b}{2}\omega \\ i &= 1 + N_1^{\mathrm{I}}, \ldots, N_2^{\mathrm{I}} \end{aligned} \tag{29}$$

where N_2^{I} is the number of the nodes for Wall 2.

Repeating the same analysis for Walls 3 and 4 yields the following results: for Wall 3

$$\begin{aligned} U^{\mathrm{I}}_{x_i} &= u - \frac{h}{2}\theta_z + \frac{bh}{b+h}\chi \\ U^{\mathrm{I}}_{y_i} &= v + x_i\theta_z + \frac{bh}{b+h}\left\{ \frac{4b}{h}\left(\frac{x_i}{b}\right)^3 - \left(\frac{b}{h}+2\right)\left(\frac{x_i}{b}\right)\right\}\chi \\ U^{\mathrm{I}}_{z_i} &= w + \frac{h}{2}\theta_x - x_i\theta_y + x_i\frac{h}{2}\omega \\ i &= 1 + N_2^{\mathrm{I}}, \ldots, N_3^{\mathrm{I}} \end{aligned} \tag{30}$$

for Wall 4

$$\begin{aligned} U^{\mathrm{I}}_{x_i} &= u - y_i\theta_z + \frac{bh}{b+h}\left\{ -\frac{4h}{b}\left(\frac{y_i}{h}\right)^3 + \left(\frac{h}{b}+2\right)\left(\frac{y_i}{h}\right)\right\}\chi \\ U^{\mathrm{I}}_{y_i} &= v - \frac{b}{2}\theta_z - \frac{bh}{b+h}\chi \\ U^{\mathrm{I}}_{z_i} &= w + y_i\theta_x + \frac{b}{2}\theta_y - y_i\frac{b}{2}\omega \\ i &= 1+N^{\mathrm{I}}_3,\ldots,N^{\mathrm{I}}_4 \end{aligned} \tag{31}$$

where N^{I}_3 and N^{I}_4 are the numbers of nodes in Walls 3 and 4, respectively. Writing Eqs. (28)–(31) into matrix form gives the components of the transformation matrix $\mathbf{T}_{\mathrm{I}}$, which are explicitly written in Appendix A.

3.2. The joint region model by a consistent joint element

In this section, we present a method to model the joint region by a joint element having degrees of freedom consistent with the 8-DOF beam theory. This section describes the procedure to estimate the joint element stiffness from the plate model of the joint region.

The joint element stiffness $\mathbf{K}^{\mathrm{J}}$ may be defined in the following equation

$$\mathbf{K}^{\mathrm{J}}\cdot\mathbf{d} = \mathbf{f} \tag{32}$$

where $\mathbf{d}$ and $\mathbf{f}$ denote the displacement and force vectors on three Interfaces I, II and III. Denoting $\mathbf{d}^j$ and $\mathbf{f}^j$ as those defined on Interface j ($j = \mathrm{I}, \mathrm{II}, \mathrm{III}$), the vectors $\mathbf{d}$ and $\mathbf{f}$ can be written as

$$\mathbf{d} = \left\{ \mathbf{d}^{\mathrm{I}} \quad \mathbf{d}^{\mathrm{II}} \quad \mathbf{d}^{\mathrm{III}} \right\}^{\mathrm{T}}$$

$$\mathbf{f} = \left\{ \mathbf{f}^{\mathrm{I}} \quad \mathbf{f}^{\mathrm{II}} \quad \mathbf{f}^{\mathrm{III}} \right\}^{\mathrm{T}}$$

The components of $\mathbf{d}^j$ and $\mathbf{f}^j$ may be found in the following definition of $\mathbf{d}^j$ and $\mathbf{f}^j$.

$$\mathbf{d}^j = \left\{ u^j \quad v^j \quad w^j \quad \theta^j_x \quad \theta^j_y \quad \theta^j_z \quad \omega^j \quad \chi^j \right\}^{\mathrm{T}}$$

$$\mathbf{f}^j = \left\{ f^j_x \quad f^j_y \quad f^j_z \quad m^j_x \quad m^j_y \quad m^j_z \quad B^j \quad Q^j \right\}^{\mathrm{T}} \quad (j = \mathrm{I}, \mathrm{II}, \mathrm{III})$$

In the T-joint in consideration, the size of the resulting stiffness matrix of the joint element is 24×24.

To determine the joint element stiffness matrix from the plate model of the joint region, the displacement field consistent with the 8-DOF beam theory is prescribed at the interfaces. The elements of the stiffness matrix may be obtained by calculating the reaction forces at the Interfaces I, II, III subjected to prescribed displacements at the interfaces.

To determine the components of the first column of $\mathbf{K}^{\mathrm{J}}$, we impose a unit displacement along the x direction on Interface I while constraining all other displacement degrees at the interfaces:

$$u^{\mathrm{I}} = 1, \quad v^{\mathrm{I}} = w^{\mathrm{I}} = \theta^{\mathrm{I}}_x = \theta^{\mathrm{I}}_y = \theta^{\mathrm{I}}_z = \omega^{\mathrm{I}} = \chi^{\mathrm{I}} = 0 \tag{33a}$$

$$\mathbf{d}^{\mathrm{II}} = \mathbf{d}^{\mathrm{III}} = 0 \tag{33b}$$

The displacement field by plate elements corresponding to Eqs. (33a) and (33b) can be written as

$$U^{\mathrm{I}}_{xi} = 1, \quad U^{\mathrm{I}}_{yi} = U^{\mathrm{I}}_{zi} = \Theta^{\mathrm{I}}_{xi} = \Theta^{\mathrm{I}}_{yi} = \Theta_{zi} = 0 \quad (i = 1,\ldots,N^{\mathrm{I}}_4) \tag{34a}$$

$$\mathbf{D}^{\mathrm{II}} = \mathbf{D}^{\mathrm{III}} = 0 \tag{34b}$$

Table 1
Displacement field imposing on the interface ($j = \mathrm{I}$)

No.	u^{I}	v^{I}	w^{I}	θ_x^{I}	θ_y^{I}	θ_z^{I}	ω^{I}	χ^{I}	U_{xi}^{I}	U_{yi}^{I}	U_{zi}^{I}	Θ_{xi}^{I}	Θ_{yi}^{I}	Θ_{zi}^{I}
1	1	0	0	0	0	0	0	0	1	0	0	0	0	0
2	0	1	0	0	0	0	0	0	0	1	0	0	0	0
3	0	0	1	0	0	0	0	0	0	0	1	0	0	0
4	0	0	0	1	0	0	0	0	0	0	y_i	1	Free	Free
5	0	0	0	0	1	0	0	0	0	0	$-x_i$	Free	1	Free
6	0	0	0	0	0	1	0	0	$-y_i$	x_i	0	Free	Free	1
7	0	0	0	0	0	0	1	0	0	0	$x_i \times y_i$	Free	Free	Free
8	0	0	0	0	0	0	0	1	$(\psi^{\chi})_{x_i}$	$(\psi^{\chi})_{y_i}$	0	0	0	0

Table 1 expresses the displacement condition imposed on Interface I, consistent with the 8-DOF beam theory. In Table 1, $(\psi^{\chi})_{x_i}$ and $(\psi^{\chi})_{y_i}$ represent the components of the distortion function ψ^{χ} in the x_i and y_i directions, respectively. In order to find the remaining components $\mathbf{K}^{\mathrm{J}}$, exactly the same procedure is repeated to impose displacement conditions on Interfaces II and III.

Once the displacement conditions are given on the interfaces, the reaction forces $\mathbf{F}^{\mathrm{I}}$, $\mathbf{F}^{\mathrm{II}}$ and $\mathbf{F}^{\mathrm{III}}$ are computed by using the plate-element model of the joint region. These forces are then converted to calculate $\mathbf{f}^{\mathrm{I}}$, $\mathbf{f}^{\mathrm{II}}$ and $\mathbf{f}^{\mathrm{III}}$ that are consistent with the 8-DOF beam theory. We use the following relations to convert $\mathbf{F}^{\mathrm{I}}$ to $\mathbf{f}^{\mathrm{I}}$:

$$f_x^{\mathrm{I}} = \sum_{i=1}^{N_4^{\mathrm{I}}} F_{xi}^{\mathrm{I}} \tag{35a}$$

$$f_y^{\mathrm{I}} = \sum_{i=1}^{N_4^{\mathrm{I}}} F_{yi}^{\mathrm{I}} \tag{35b}$$

$$f_z^{\mathrm{I}} = \sum_{i=1}^{N_4^{\mathrm{I}}} N_{zi}^{\mathrm{I}} \tag{35c}$$

$$m_x^{\mathrm{I}} = \sum_{i=1}^{N_4^{\mathrm{I}}} F_{zi}^{\mathrm{I}} \times y_i + M_{xi}^{\mathrm{I}} \tag{35d}$$

$$m_y^{\mathrm{I}} = \sum_{i=1}^{N_4^{\mathrm{I}}} F_{zi}^{\mathrm{I}} \times (-x_i) + M_{yi}^{\mathrm{I}} \tag{35e}$$

$$m_z^{\mathrm{I}} = \sum_{i=1}^{N_4^{\mathrm{I}}} F_{si}^{\mathrm{I}} \times r_i + M_{zi}^{\mathrm{I}} \tag{35f}$$

$$B^{\mathrm{I}} = \sum_{i=1}^{N_4^{\mathrm{I}}} F_{zi}^{\mathrm{I}} \times x_i \times y_i \tag{35g}$$

$$Q^{\mathrm{I}} = \sum_{i=1}^{N_4^{\mathrm{I}}} \left[F_{si}^{\mathrm{I}} \times \psi_s^{\chi}(s_i) \right] \pm M_{zi} \tag{35h}$$

In Eq. (35f), F_{si}^{I} stands for the force acting along the tangential direction s_i on Interface I (see Fig. 1 for the positive tangential directions s_i). Similar definitions hold for quantities associated with other interfaces. Once all components of $\mathbf{f}^{\mathrm{I}}$, $\mathbf{f}^{\mathrm{II}}$, and $\mathbf{f}^{\mathrm{III}}$ are determined, the components of $\mathbf{K}^{\mathrm{J}}$ are simply found as

$$(\mathbf{K}^{\mathrm{J}})_{1,k} = f_x^{\mathrm{I}}, \quad (\mathbf{K}^{\mathrm{J}})_{2,k} = f_y^{\mathrm{I}}, \quad (\mathbf{K}^{\mathrm{J}})_{3,k} = f_z^{\mathrm{I}}, \ldots, (\mathbf{K}^{\mathrm{J}})_{24,k} = f_\chi^{\mathrm{III}} \quad (\text{for } \mathbf{d} = 0 \text{ except } \mathbf{d}_k \neq 0)$$

For a dynamic analysis, we construct the mass matrix $\mathbf{M}^{\mathrm{J}}$ of the joint element using the Guyan reduction method (see Guyan, 1965). Since the Guyan method is well known, the detailed procedure to construct $\mathbf{M}^{\mathrm{J}}$ will not be given here. However, we remark that the mass components of the joint region are transferred to those defined on the interfaces. The transferred mass components are then converted to those consistent with the 8-DOF beam theory (see Kim, 1998).

4. Numerical results

4.1. Case study 1: effects of the joint region size

We perform the vibration analysis for a T-joint thin-walled structure shown in Fig. 3 ($L = 475$ mm, $b = h = 50$ mm, $t = 1$ mm, Young's modulus $E = 2 \times 10^{11}$ N/m^3, mass density $\rho = 7.8 \times 10^{-6}$ kg/mm^3). Table 2 shows the eigenfrequencies of a freely supported T-joint for varying values of the size L_j of the joint region. 'Plate' denotes the results by the detailed plate-element analysis. 'Plate + 8-DOF beam' denotes the model using plate elements for the joint region and 8-DOF beam elements for the box beams. Observe that the present results are little affected by the size L_j. However, the existing literature (see, e.g., Kim et al., 1995) reports inconsistency when conventional six-degree-of-freedom beam elements are employed to model box beams.

4.2. Case study 2: performance of the present approaches

Table 3 presents the eigenfrequencies for the same T-joint used in Case study 1. In Table 3, the eigenfrequencies predicted by four different methods are compared. 'Plate + 6-DOF beam' represents the model

Table 2
Effects of the size L_j of the joint region for Case study 1 (N_e: number of the finite elements)

Mode no.	Plate ($N_e = 1872$) (Hz)	Plate + 8-DOF beam $L_j = 25$ mm (Hz)	Plate + 8-DOF beam $L_j = 50$ mm (Hz)	Plate + 8-DOF beam $L_j = 75$ mm (Hz)
1	212.2	224.7	223.3	223.4
2	277.5	287.0	286.1	286.1
3	292.1	288.3	288.6	289.6
4	300.2	293.1	293.6	296.1

Table 3
Eigenfrequencies of a T-joint thin-walled structure obtained by various modeling techniques (Case study 2)

Mode no.	Plate ($N_e = 1872$) (Hz)	Plate + 6-DOF beams $L_j = 50$ mm (Hz)	Plate + 8-DOF beams $L_j = 50$ mm (Hz)	Joint + 8-DOF beams $L_j = 25$ mm (Hz)
1	212.2	223.2	223.3	217
2	277.5	285.6	286.1	288
3	292.1	N/A	288.6	294
4	300.2	N/A	293.6	353

utilizing plate elements for the joint region and conventional six-degree-of-freedom beam elements for the box beams. 'Joint + 8-DOF beam' is the model using the joint element ($\mathbf{K}^J$, $\mathbf{M}^J$) for the joint region and 8-DOF beam elements for the box beams. The number of the 8-DOF beam elements used to model the three adjacent box beams is 51. The element used here is similar to that developed by Kim and Kim (1999a,b). The convergence of results has been checked numerically.

Table 3 shows that 'Plate + 6-DOF beam' cannot predict the third and fourth eigenmodes although their eigenfrequencies are low enough to be close to the second lowest eigenfrequency. However, the present approaches ('Plate + 8-DOF beam', 'Joint + 8-DOF beam') can predict well all of the lowest four eigenmodes. It is observed that the third and fourth mode shapes have significant warping and distortional deformations, which are well seen in Figs. 5 and 6. We also remark that the distortional deformations significant particularly near the joint region are well captured by the present approaches.

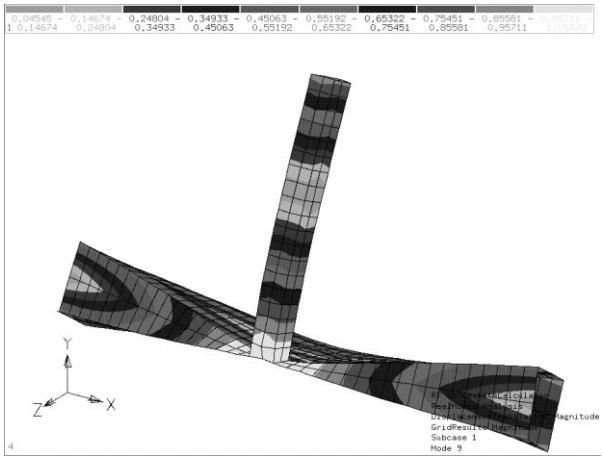

(a)

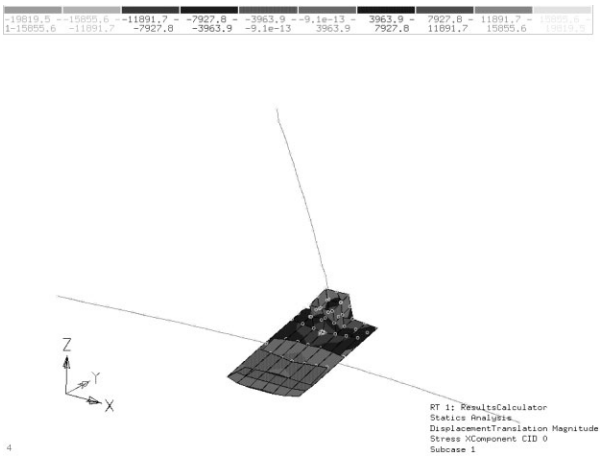

(b)

Fig. 5. The third eigenmode of the T-joint modeled (a) by plate elements and (b) by the combination of plate and 8-DOF beam elements.

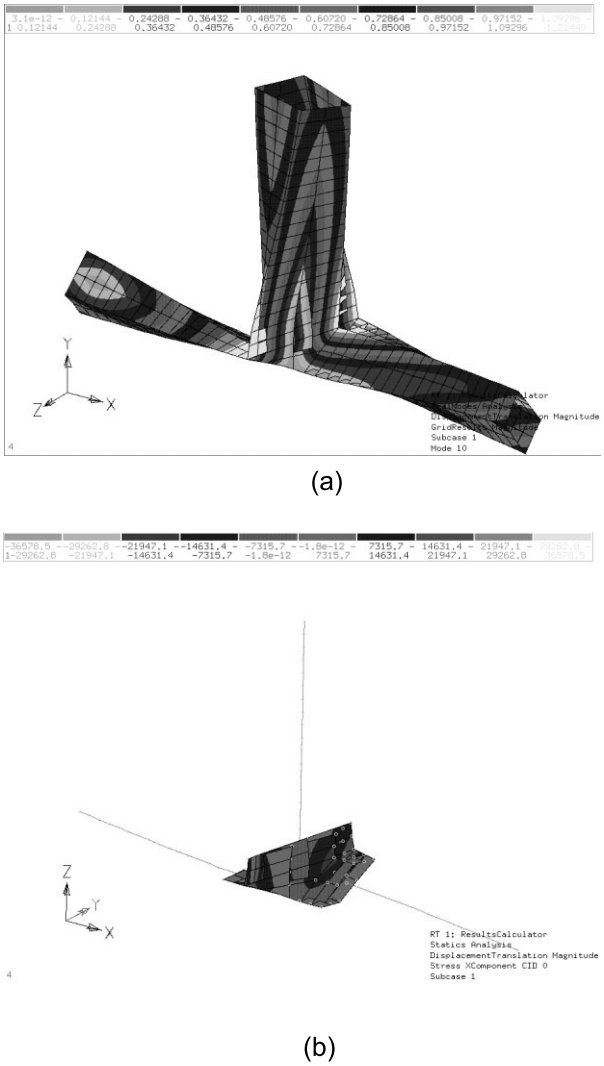

Fig. 6. The fourth eigenmode of the T-joint modeled (a) by plate elements and (b) the combination of plate and 8-DOF beam elements.

5. Conclusions

We have proposed new efficient modeling techniques for T-joint thin-walled structures based on the 8-DOF beam theory. The key essence of the present method was (i) to use beam theories that facilitate early designs, but (ii) to use an 8-DOF beam theory for accurate, reliable results. This work showed that the significant contributions of warping and distortional deformations near the joint region of a T-joint can be well accommodated by the present 8-DOF beam theory. Without the present beam theory, it is not possible to predict important low-frequency vibration modes only with conventional beam theories. The use of additional degrees of freedom for warping and distortion is well compensated by greatly improved results. Though this work is limited to a simple T-joint structure, the present finding as well

as analysis can be carried over to the analysis of joints consisting of arbitrarily-sectioned thin-walled beams.

Appendix A

$$[\mathbf{T}_{\mathrm{I}}] = \begin{bmatrix} \mathbf{T}_{\mathrm{I1}} \\ \mathbf{T}_{\mathrm{I2}} \\ \mathbf{T}_{\mathrm{I3}} \\ \mathbf{T}_{\mathrm{I4}} \end{bmatrix}$$

where

$$\mathbf{T}_{\mathrm{I1}} = \begin{bmatrix} 1 & 0 & 0 & 0 & 0 & \frac{h}{2} & 0 & -\frac{bh}{b+h} \\ 0 & 1 & 0 & 0 & 0 & x_1 & 0 & \frac{bh}{b+h}\left\{-\frac{4b}{h}\left(\frac{x_1}{b}\right)^3 + \left(\frac{b}{h}+2\right)\left(\frac{x_1}{b}\right)\right\} \\ 0 & 0 & 1 & -\frac{h}{2} & -x_1 & 0 & -\frac{h}{2}x_1 & 0 \\ & & & & \vdots & & & \\ 1 & 0 & 0 & 0 & 0 & \frac{h}{2} & 0 & -\frac{bh}{b+h} \\ 0 & 1 & 0 & 0 & 0 & x_{N_1^{\mathrm{I}}} & 0 & \frac{bh}{b+h}\left\{-\frac{4b}{h}\left(\frac{x_{N_1^{\mathrm{I}}}}{b}\right)^3 + \left(\frac{b}{h}+2\right)\left(\frac{x_{N_1^{\mathrm{I}}}}{b}\right)\right\} \\ 0 & 0 & 1 & -\frac{h}{2} & -x_{N_1^{\mathrm{I}}} & 0 & -\frac{h}{2}x_{N_1^{\mathrm{I}}} & 0 \end{bmatrix}$$

$$\mathbf{T}_{\mathrm{I2}} = \begin{bmatrix} 1 & 0 & 0 & 0 & 0 & -y_{1+N_1^{\mathrm{I}}} & 0 & \frac{bh}{b+h}\left\{\frac{4h}{b}\left(\frac{y_{1+N_1^{\mathrm{I}}}}{h}\right)^3 - \left(\frac{h}{b}+2\right)\left(\frac{y_{1+N_1^{\mathrm{I}}}}{h}\right)\right\} \\ 0 & 1 & 0 & 0 & 0 & \frac{b}{2} & 0 & \frac{bh}{b+h} \\ 0 & 0 & 1 & y_{1+N_1^{\mathrm{I}}} & -\frac{b}{2} & 0 & \frac{b}{2}y_{1+N_1^{\mathrm{I}}} & 0 \\ & & & & \vdots & & & \\ 1 & 0 & 0 & 0 & 0 & -y_{N_2^{\mathrm{I}}} & 0 & \frac{bh}{b+h}\left\{\frac{4h}{b}\left(\frac{y_{N_2^{\mathrm{I}}}}{h}\right)^3 - \left(\frac{h}{b}+2\right)\left(\frac{y_{N_2^{\mathrm{I}}}}{h}\right)\right\} \\ 0 & 1 & 0 & 0 & 0 & \frac{b}{2} & 0 & \frac{bh}{b+h} \\ 0 & 0 & 1 & y_{N_2^{\mathrm{I}}} & -\frac{b}{2} & 0 & \frac{b}{2}y_{N_2^{\mathrm{I}}} & 0 \end{bmatrix}$$

$$\mathbf{T}_{\mathrm{I3}} = \begin{bmatrix} 1 & 0 & 0 & 0 & 0 & -\frac{h}{2} & 0 & \frac{bh}{b+h} \\ 0 & 1 & 0 & 0 & 0 & x_{1+N_2^{\mathrm{I}}} & 0 & \frac{bh}{b+h}\left\{\frac{4b}{h}\left(\frac{x_{1+N_2^{\mathrm{I}}}}{b}\right)^3 - \left(\frac{b}{h}+2\right)\left(\frac{x_{1+N_2^{\mathrm{I}}}}{b}\right)\right\} \\ 0 & 0 & 1 & \frac{h}{2} & -x_{1+N_2^{\mathrm{I}}} & 0 & \frac{h}{2}x_{1+N_2^{\mathrm{I}}} & 0 \\ & & & & \vdots & & & \\ 1 & 0 & 0 & 0 & 0 & -\frac{h}{2} & 0 & \frac{bh}{b+h} \\ 0 & 1 & 0 & 0 & 0 & x_{N_3^{\mathrm{I}}} & 0 & \frac{bh}{b+h}\left\{\frac{4b}{h}\left(\frac{x_{N_3^{\mathrm{I}}}}{b}\right)^3 - \left(\frac{b}{h}+2\right)\left(\frac{x_{N_3^{\mathrm{I}}}}{b}\right)\right\} \\ 0 & 0 & 1 & \frac{h}{2} & -x_{N_3^{\mathrm{I}}} & 0 & \frac{h}{2}x_{N_3^{\mathrm{I}}} & 0 \end{bmatrix}$$

$$\mathbf{T}_{I4}=\begin{bmatrix}
1 & 0 & 0 & 0 & 0 & -y_{1+N_3^I} & 0 & \frac{bh}{b+h}\left\{-\frac{4h}{b}\left(\frac{y_{1+N_3^I}}{h}\right)^3+\left(\frac{h}{b}+2\right)\left(\frac{y_{1+N_3^I}}{h}\right)\right\}\\
0 & 1 & 0 & 0 & 0 & -\frac{b}{2} & 0 & -\frac{bh}{b+h}\\
0 & 0 & 1 & y_{1+N_3^I} & \frac{b}{2} & 0 & -\frac{b}{2}y_{1+N_3^I} & 0\\
 & & & & \vdots & & & \\
1 & 0 & 0 & 0 & 0 & -y_{N_4^I} & 0 & \frac{bh}{b+h}\left\{-\frac{4h}{b}\left(\frac{y_{N_4^I}}{h}\right)^3+\left(\frac{h}{b}+2\right)\left(\frac{y_{N_4^I}}{h}\right)\right\}\\
0 & 1 & 0 & 0 & 0 & -\frac{b}{2} & 0 & -\frac{bh}{b+h}\\
0 & 0 & 1 & y_{N_4^I} & \frac{b}{2} & 0 & -\frac{b}{2}y_{N_4^I} & 0
\end{bmatrix}$$

References

Altenbach, J., 1991. Finite element modelling and analysis of thinwalled structures. In: The Mathematics of Finite Elements and Applications VII London. Academic Press, London.

Altenbach, J., Kissing, W., Altenbach, H., 1994. Dunnwandige Stab-und Stabschalentragwerke Braunschweig. Vieweg, Wiesbaden.

Balch, C.D., Steele, C.R., 1987. Asymptotic solutions for warping and distortion of thin-walled box beams. ASME Journal of Applied Mechanics 54, 165–173.

Bjerhammar, A., 1973. Theory of Errors and Generalized Matrix Inverse. Elsevier Scientific Publishing Company, New York.

Chang, D.C., 1974. Effects of flexible connections on body structural response. SAE Transactions 83, 233–244.

El-sayed, M.E.M., 1989. Calculation of joint spring rates using finite element formulation. Computers and Structures 33 (4), 977–981.

Garro, L., Vullo, V., 1986. Deformations car body joints under operating conditions. SAE 863197, pp. 5403–5420.

Guyan, R.J., 1965. Reduction of stiffness and mass matrices. AIAA Journal 3, 380.

Kim, D.W., 1998. A study on the higher-order joint stiffness for the vibration analysis of thin-walled beam structures. Master Thesis, Department of Mechanical Design and Production Engineering, Seoul National University, Seoul Korea.

Kim, H.S., 1997. A technique to match different finite elements in the vibration analysis of a T-joint. Master Thesis, Department of Mechanical Design and Production Engineering, Seoul National University, Seoul Korea.

Kim, J.H., Kim, Y.Y., 1999a. Analysis of thin-walled closed beams with general quadrilateral cross sections. ASME Journal of applied mechanics 66 (4), 904–912.

Kim, J.H., Kim, Y.Y., 2000. One-dimensional analysis of thin-walled closed beams having general cross sections. International Journal for Numerical Methods in Engineering 49, 653–668.

Kim, Y.Y., Kim, J.H., 1999b. Thin-walled closed box beam element for static and dynamic analysis. International Journal for Numerical Methods in Engineering 45, 473–490.

Kim, Y.Y., Yim, H.J., Kang, J.H., Kim, J.H., 1995. Reconsideration of the joint modelling technique: in a box-beam T-joint. SAE 951108, pp. 275–279.

Lubkin, J.L., 1974. The flexibility of a tubular welded joint in a vehicle frame. SAE 740340, pp. 1518–1522.

Lee, K., Nikolaidis, E., 1992. A two-dimensional model for joints in vehicle structures. Computers and Structures 45 (4), 775–784.

Sunami, Y., Yugawa, T., Yoshida, Y., 1988. Analysis of joint rigidity in-plane bending of plane-joint structures. JSAE Review 9 (2), 44–51.

Sunami, Y., Yugawa, T., Yoshida, Y., 1990. Analysis of joint rigidity of the automotive body structure-out-of-plane bending of plane-joint structures. JSAE Review 11 (3), 59–66.

Vlasov, V.Z., 1961. Thin walled elastic beams. Israel Program for Scientific Translations, Jerusalem.